npg

ATM-dependent expression of IEX-1 controls nuclear accumulation of Mcl-1 and the DNA damage response

P Pawlikowska[1,2,3], I Leray[1,2,3], B de Laval[1,2,3], S Guihard[1,2,3], R Kumar[4], F Rosselli[5] and F Porteu*[1,2,3]

The early-response gene product IEX-1 (also known as IER3) was recently found to interact with the anti-apoptotic Bcl-2 family member, myeloid cell leukemia-1 (Mcl-1). In this study we show that this interaction specifically and timely controls the accumulation of Mcl-1 in the nucleus in response to DNA damage. The IEX-1 protein is rapidly induced by γ-irradiation, genotoxic agents or replication inhibitors, in a way dependent on ataxia telangiectasia mutated (ATM) activity and is necessary for Mcl-1 nuclear translocation. Conversely, IEX-1 protein proteasomal degradation triggers the return of Mcl-1 to the cytosol. IEX-1 and Mcl-1 are integral components of the DNA damage response. Loss of IEX-1 or Mcl-1 leads to genomic instability and increased sensitivity to genotoxic and replicative stresses. The two proteins cooperate to maintain Chk1 activation and G2 checkpoint arrest. Mcl-1 nuclear translocation may foster checkpoint and improve the tumor resistance to DNA damage-based cancer therapies. Deciphering the pathways involved in IEX-1 degradation should lead to the discovery of new therapeutic targets to increase sensitivity of tumor cells to chemotherapy.
Cell Death and Differentiation (2010) **17,** 1739–1750; doi:10.1038/cdd.2010.56; published online 14 May 2010

Cells respond to DNA damage by activating a protein network that recognizes the damaged DNA, triggering cell cycle checkpoints, repair of the damaged DNA and/or cell death. The DNA damage response (DDR) is regulated by two primary signaling pathways activated downstream of the effector kinases, ataxia-telangiectasia mutated (ATM) and ATM-and Rad3-related (ATR), which are mutated in ataxia-telangiectasia and Seckel syndrome, respectively. ATM is activated in response to agents inducing DNA double-strand breaks (DSBs), whereas ATR responds to a broad spectrum of genotoxic stresses. In the presence of DSBs, the Mre11/Rad50/Nbs1 complex accumulates at DNA-damage sites, forming subnuclear foci. Recruitment of ATM to this complex fosters its activation, leading to phosphorylation of numerous substrates, including the histone H2AX that serves as a scaffold for the recruitment of DNA repair and checkpoint signaling proteins. ATM triggers the processing of DSBs into extended regions of single-stranded DNA. ATR is then recruited and activated to RPA-coated ssDNA. ATM and ATR phosphorylate the checkpoint kinases Chk1 and Chk2, respectively, which will give cell the time to repair the damaged DNA by arresting their cycle at the G1-S or G2-M transitions and within the S phase.[1]

In the face of irreparable damage the cell may activate its apoptotic machinery. On the contrary, in response to low levels of damage and during the checkpoint arrests, apoptosis needs to be suppressed to allow repair and avoid unnecessary cell destruction. The correct balance between cell cycle arrest and apoptosis is crucial to ensure genomic stability. This suggests a high and complex interplay between proteins controlling the DDR and the apoptotic pathways. Evolutionary conserved Bcl-2 family members are central regulators of apoptosis. Myeloid cell leukemia-1 (Mcl-1) is an anti-apoptotic member of this family. Models of Mcl-1 knock-out mice have shown its requirement for embryonic development and differentiation of various hematopoietic lineages.[2–4] Mcl-1 is regulated at transcriptional, post-transcriptional and post-translational levels.[5,6] Its anti-apoptotic function is regulated by interaction with other Bcl-2 family members.[7] Outside of this family, Mcl-1 interacts with proteins regulating apoptosis or cell proliferation, including fortilin, cdk1 and PCNA.[8–10] Recent studies have identified immediate early-response gene X-1 (IEX-1, also known as IER3) as a new partner of Mcl-1.[11,12] IEX-1 is an early-response gene product that is rapidly induced by growth factors, ionizing radiations and viral infections. Conflicting data have been reported concerning its role in survival: IEX-1 was found to not only increase apoptosis in response to TNF-α,[11,13–15] but also to contribute to growth factor-mediated survival[15,16] and to prevent activation-induced T-cell death.[17,18] Other functions have been attributed to IEX-1 such as regulation of ERK, Akt and NF-κB signaling pathways.[14,16,19]

Unlike a previous report,[12] we found that although IEX-1 and Mcl-1 inhibit staurosporin-induced apoptosis, this function

is independent of their interaction. A recent study reported that Mcl-1 translocates to the nucleus after treatment with etoposide.[20] In this study we show that Mcl-1 nuclear translocation is a general response to genotoxic stress and that it is strictly and timely controlled by IEX-1. IEX-1 expression is rapidly induced by DNA-damaging agents in an ATM-dependent manner and is necessary for Mcl-1 nuclear translocation. Conversely, IEX-1 protein degradation triggers Mcl-1 return to the cytosol. IEX-1 and Mcl-1 are integral components of the DDR pathway. They cooperate to maintain Chk1 activation, and regulate proper G2 checkpoint arrest and repair of DNA lesions and cell survival after treatments with various DNA-damaging agents.

Results

Mcl-1 nuclear accumulation is induced by genotoxic stress and is controlled by IEX-1.

Anti-HA antibodies could immunoprecipitate Mcl-1 but not Bcl-2 from cells transfected with HA-IEX-1 and either Myc-Mcl-1 or Flag-Bcl-2 (Figure 1a and Supplementary Figure S1-a). Immunofluorescence (IF) analysis revealed that expression of GFP-IEX-1 induced a striking accumulation of endogenous Mcl-1, but not of Bcl-2 or Bcl-xL, to the nucleus (Figure 1b and Supplementary Figure S1-b). Measurement of mean pixel intensities in the nucleus and in the cytoplasm of random cells showed that Mcl-1, but not Bcl-2 or Bcl-xL, was enriched in the nucleus of the cells overexpressing GFP-IEX-1 (Supplementary Figure S1-c). IEX-1 possesses a nuclear localization signal (NLS) and a putative transmembrane (TM) region.[15,21,22] Deletion of IEX-1 NLS prevented Mcl-1 nuclear accumulation but not Mcl-1/IEX-1 interaction (Supplementary Figure S1a and b) whereas deletion of IEX-1 TM (IEX-1-ΔTM) abolished both events (Figures 1a and b). Thus, IEX-1-induced Mcl-1 nuclear accumulation is dependent on its interaction with Mcl-1 and requires an intact NLS.

Endogenous IEX-1 expression and Mcl-1 nuclear accumulation were conjointly induced by a variety of DNA-damaging agents such as etoposide, ionizing radiations (IRs) and the replicative inhibitor hydroxyurea (HU) (Figure 1c). IEX-1 could be detected by IF as soon as 30 min after IR (data not shown). The Mcl-1 nuclear/cytoplasmic (N/C) IF intensity ratio was increased in the nucleus of all cells after IR (0.87 ± 0.016 and 1.8 ± 0.06 for non-treated and IR-treated cells, respectively, Supplementary Figure S1-c). Confirming these results, cell fractionation indicated that the nucleus of resting cells contains 15% (N/C ratio of 0.18) of total Mcl-1, whereas this level reached up to 40% (N/C ratio of 0.8) after IR or HU (Figure 1d). Neither IEX-1 overexpression nor DNA damage had any effect on total Mcl-1 levels or half-life (Figure 1d and Supplementary Figure S1-d).

Endogenous IEX-1 and Mcl-1 colocalized in the nucleus and could be co-immunoprecipitated from the nuclear fraction of HeLa cells after HU or IR treatments (Figures 1c and e). IF analysis in cells subjected to detergent extraction before fixation showed that although the global intensity of the signal was greatly decreased under these conditions, most of the IR-treated cells stained positively for nuclear Mcl-1 and IEX-1 (Figure 1f). In contrast, the Mcl-1 signal was entirely lost in non-treated cells. This further supports Mcl-1 delocalization upon IR and indicates that IEX-1 and Mcl-1 associate, at least partially, with the chromatin fraction after DNA damage.

HeLa cells expressing IEX-1 short hairpin RNAs (shRNAs)[23] showed a great decrease in both IEX-1 induction and Mcl-1 nuclear accumulation upon HU or IR treatment (Figures 2a and b). Fractionation experiments showed that IR increased Mcl-1 levels in the nuclear fraction of cells expressing scramble but not IEX-1 shRNAs (Figure 2c). Moreover, although in IEX-1$^{+/+}$ hematopoietic progenitors Mcl-1 had entirely moved from the cytoplasm to the nucleus 3 h after IR, its localization remained unchanged in IEX-1$^{-/-}$ cells (Figure 2d). Expression of IEX-1 in IEX-1$^{-/-}$ mouse embryonic fibroblasts (MEFs) restored IR-mediated Mcl-1 nuclear staining (Supplementary Figure S2). Thus, IEX-1 induction is a prerequisite for IR-induced Mcl-1 nuclear translocation.

ATM activity is required for IEX-1 expression and to maintain Mcl-1 in the nucleus.

Both IR- or HU-mediated IEX-1 expression and Mcl-1 nuclear accumulation were abolished in ATM-deficient GM3189 lymphoblastoid cells and upon treatment of HeLa cells with the ATM inhibitors caffeine and KU-55933 (Figures 3a and b), showing that these events require ATM activity.

IEX-1 is a short half-life protein, sensitive to degradation by the proteasome. In cells treated overnight with HU and then released in HU-free medium, IEX-1 staining was strong at 5 h, started to fade at 9 h and disappeared at 16 h (Figure 3c). Mcl-1 localized to the nucleus as long as IEX-1 was present and returned to the cytosol when IEX-1 vanished. Addition of the proteasome inhibitor, *N*-acetyl-Leu-Leu-NorLeu-al (LLnL), at 5 h prevented IEX-1 disappearance and Mcl-1 nuclear exit. In the absence of HU, treatment with LLnL alone for 4 h did not induce IEX-1. In agreement with previous reports,[5,6] Mcl-1 expression increased slightly under these conditions but it remained mostly located in the cytoplasm. No apoptosis could be detected up to 16 h, showing that neither the nuclear localization of Mcl-1 nor its relocalization to the cytosol is linked to cell death. Thus, IEX-1 is necessary to both bring and maintain Mcl-1 into the nucleus.

To determine whether ATM activity is required to maintain IEX-1 expression once induced, the cells were synchronized, arrested in G2 by IR and then treated with caffeine or KU-55933.[24] Inhibition of ATM activity accelerated IEX-1 degradation and triggered Mcl-1 nuclear exit (Figure 3d), showing that IEX-1 induction and degradation, as well as the subsequent nucleo-cytoplasmic movement of Mcl-1, are DNA damage- and ATM-controlled events.

Mcl-1-deficient cells show prolonged DNA damage and impaired DNA repair.

To assess the role of Mcl-1 in the DDR, we first monitored the extent of DNA damage by analyzing the presence of γ-H2AX foci. At 30 min after HU treatment, most Mcl-1$^{+/+}$ and Mcl-1$^{-/-}$ MEFs presented γ-H2AX foci. However, γ-H2AX staining declined more rapidly in wild-type (WT) than in Mcl-1$^{-/-}$ cells (Figure 4a and Supplementary Figure S3-a). Mcl-1$^{-/-}$ MEFs regained normal γ-H2AX foci disappearance kinetics upon infection with a Mcl-1-encoding but not with an empty vector. The slower removal of γ-H2AX foci, indicative of prolonged DNA
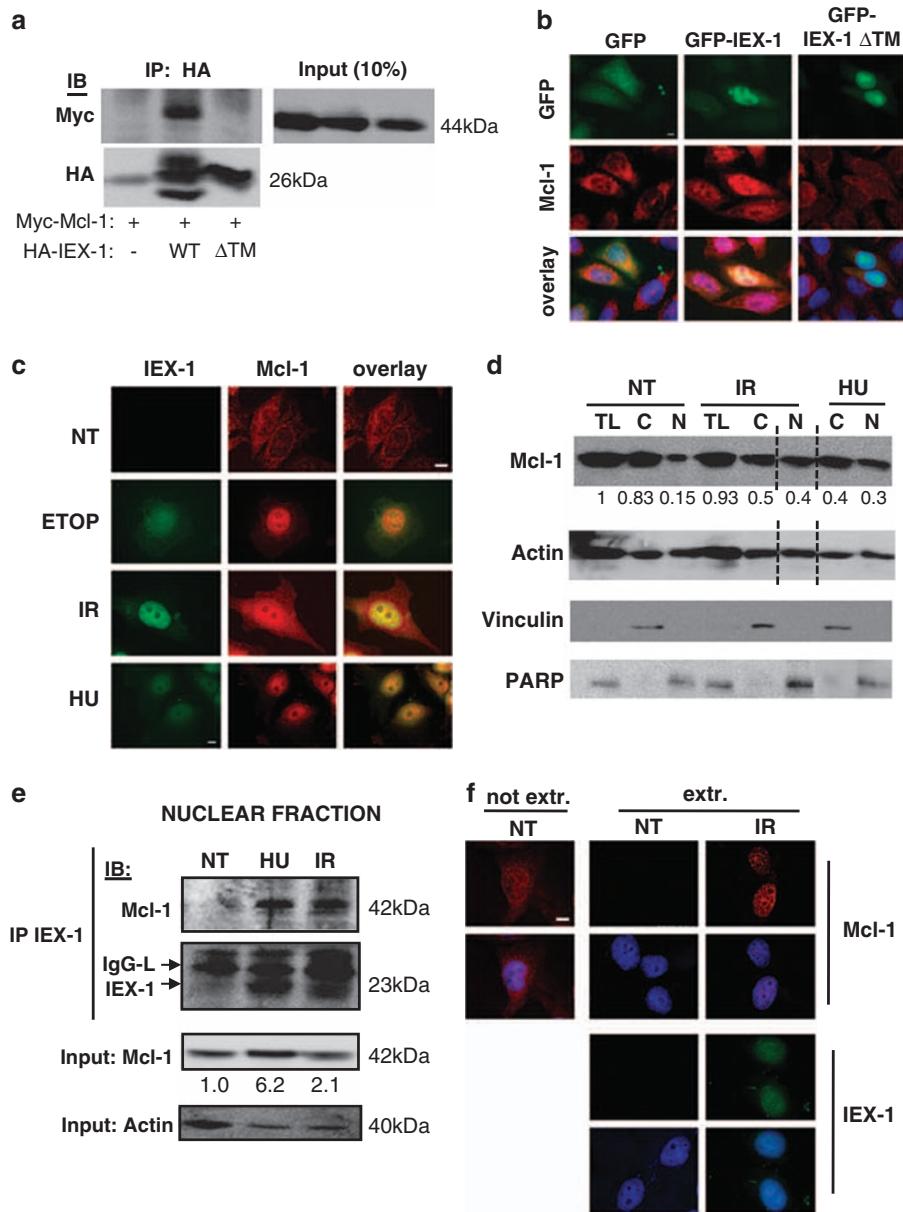
Figure 1 IEX-1 protein expression and Mcl-1 nuclear accumulation are conjointly induced by DNA damage. (**a**) CHO cells were transfected with Myc-Mcl-1 with or without HA-IEX-1 WT or ΔTM. Anti-HA immunoprecipitates (IP) and total lysates (input) were immunoblotted (IB) with the indicated antibodies. (**b**) HeLa cells transfected with GFP, GFP-IEX-1 WT or ΔTM were stained with anti-Mcl-1 (red) and counterstained with DAPI (blue). (**c**) HeLa cells were untreated (NT) or treated with etoposide (100 μM, 4 h), IR (10 Gy, 6 h) or HU (2.5 mM, 4 h), fixed and stained with anti-IEX-1 (green) and anti-Mcl-1 (red). (**d**, **e**) HeLa cells were treated as in (**c**). One part of the cells was used for total lysates (TL) and the other part was fractionated. TL, cytosolic (C) and nuclear (N) extracts were directly loaded on SDS gels (**d**) or IP with anti-IEX-1 antibodies (**e**). Input: 10% of nuclear extracts. Mcl-1 quantifications, normalized to actin levels, are expressed relative to the levels in NT cells. The results shown in **d** come from a unique blot that was cutoff (dotted line). (**f**) HeLa cells were not treated (NT) or irradiated (10 Gy). After 6 h, the soluble proteins were extracted (extr.) or not (not extr.) before fixation and staining with anti-Mcl-1 (red) or anti-IEX-1 (green). Nuclei were counterstained with DAPI. Bars, 10 μm

damage, was also found after irradiation of shMcl-1-expressing HeLa cells (Supplementary Figure S3-b).

Persistent DNA damage may result from defects in DNA repair, cell cycle checkpoints or both. To analyze the first possibility, we performed comet assays. DNA breaks are visible by increased DNA mobility or 'comet tails'. The comet tail moment was measured to quantify the extent of unrepaired DNA. Just after irradiation, all the cells showed

comparable amounts of DNA breaks. However, 1 h later, Mcl-1$^{+/+}$ MEFs had rejoined 74% of the breaks, whereas 63% of them remained unrepaired in Mcl-1$^{-/-}$ cells. This defect was completely restored upon re-expression of Mcl-1 in Mcl-1$^{-/-}$ cells (Figure 4b). Interestingly, non-treated-Mcl-1$^{-/-}$ cells had a basal tail moment slightly but reproducibly higher than control cells, showing that they contain unresolved DNA damage. This suggests that Mcl-1 could have a role in the
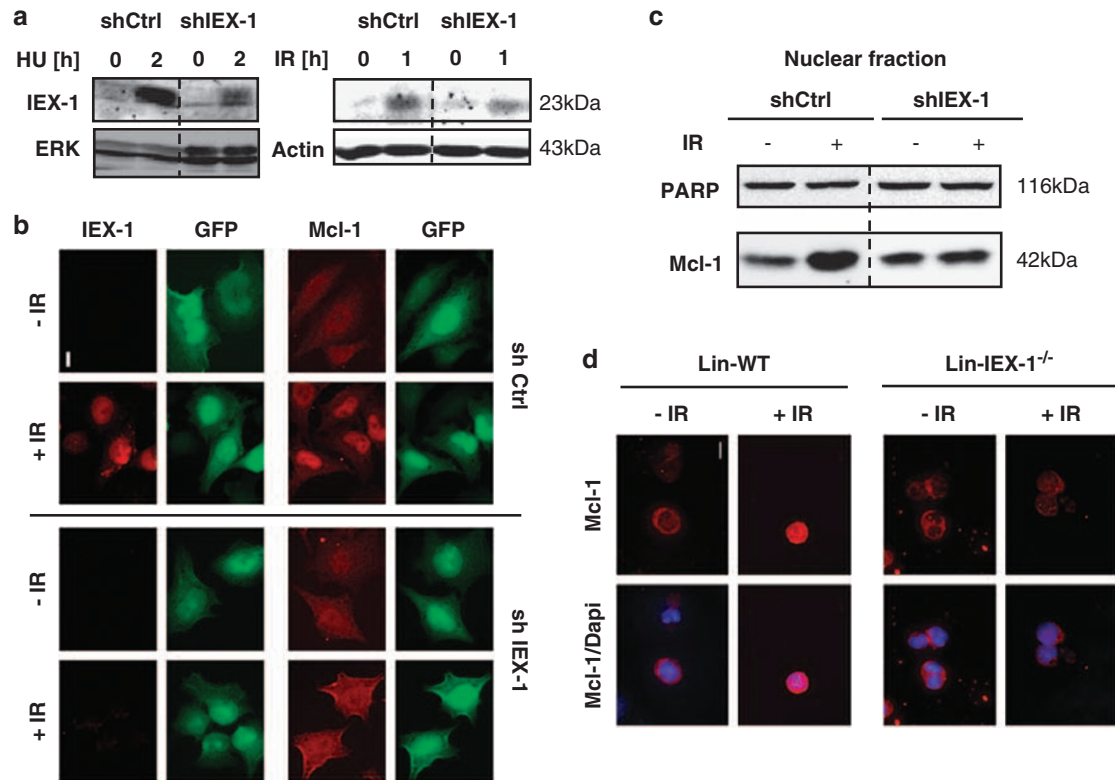
Figure 2 DNA damage-induced Mcl-1 nuclear localization depends on IEX-1 expression. (**a**–**c**) HeLa cells were infected with lentiviruses encoding scramble or IEX-1 shRNAs and GFP and treated with HU or IR (10 Gy). (**a**) Total lysates were assessed for IEX-1 expression by IB. (**b**) The cells were fixed and stained either with anti-IEX-1 (red) or Mcl-1 antibodies (red). GFP (green) indicates infected cells. (**c**) Nuclear extracts were prepared, treated with formaldehyde and analyzed by IB. (**d**) IEX-1$^{-/-}$ or WT Lin$^-$ progenitors were irradiated with 10 Gy, fixed 3 h later, and stained with anti Mcl-1 antibody and DAPI. Bars, 10 μm

repair of both induced and spontaneous DNA damage occurring during normal DNA replication.

Mcl-1 deficiency leads to impaired Chk1 phosphorylation and G2/M arrest. To get insights into the mechanisms by which Mcl-1 influences the DDR, we examined whether its expression affected DNA damage signaling. ATM phosphorylation was not decreased but was rather more pronounced in shMcl-1-expressing HeLa cells (Figure 5a). The loss of Mcl-1 led to a decreased IR-induced Chk1 phosphorylation on serines 296, 345 and 317, the three sites targeted by ATR (Figures 5a and b). This effect was particularly striking at longer time points, suggesting that Mcl-1 is not required to activate Chk1 but to maintain its activity. No decrease in the phosphorylation of the other ATM/ATR substrates, Chk2, RPA32, Rad17, SMC1 and NBS1, could be observed. The prolonged phosphorylation of H2AX confirmed the sustained presence of γ-H2AX foci in Mcl-1-deficient cells. These data suggest that Mcl-1 contributes to DDR by maintaining selectively Chk1 activation.

Chk1 is required for intra-S and G2/M checkpoint activation. To analyze both phases of the cell cycle, the cells were doubly labeled with BrdU and propidium iodide (PI). Inhibition of Mcl-1 expression had no effect on the unperturbed cell cycle (Figure 5c). IR induced accumulation of control cells in the S and G2 phases of the cell cycle. Mcl-1 downregulation had no effect on the S-phase progression or on the accumulation

in G2 until 6 h after IR. However, at 24 h after IR, although control cells were still blocked in G2, shMcl-1-expressing cells had already started to re-enter in G1. A similar shorter G2 arrest was observed in Mcl-1-deficient MEFs (Supplementary Figure S3-c). Thus, Mcl-1 is indispensable to maintain Chk1 phosphorylation and the G2 checkpoint, allowing correct DNA repair in response to DNA damage.

IEX-1- and Mcl-1 act on the same pathway to regulate the DDR. HeLa cells expressing IEX-1-shRNA, as well as IEX-1$^{-/-}$ MEFs, showed spontaneous DNA breakage and, after IR, sustained γ-H2AX staining, delayed repair of DSBs (Figure 6a and Supplementary Figure S4-a), reduced length of the G2/M arrest (Figure 6b) and decreased Chk1 phosphorylation (Figure 6c and Supplementary Figure S4-b). Infection of IEX-1$^{-/-}$ MEFs with IEX-1-encoding vector rescued completely the kinetics of γ-H2AX foci removal and of DNA repair in response to IR (Figure 6a and Supplementary Figure S4-a). Thus, IEX-1 deficiency recapitulates Mcl-1 deficiency, suggesting that the two proteins act on the same pathway in the DDR. In agreement with this hypothesis, IEX-1$^{-/-}$ cells expressing the IEX-1-ΔTM mutant, which fails to interact with Mcl-1, behaved as IEX-1$^{-/-}$ cells transfected with GFP (Figure 6a and Supplementary Figure S4-a). Moreover, expression of IEX-1 could rescue the kinetics of disappearance of γ-H2AX foci in HeLa cells expressing shIEX-1 but not in cells expressing
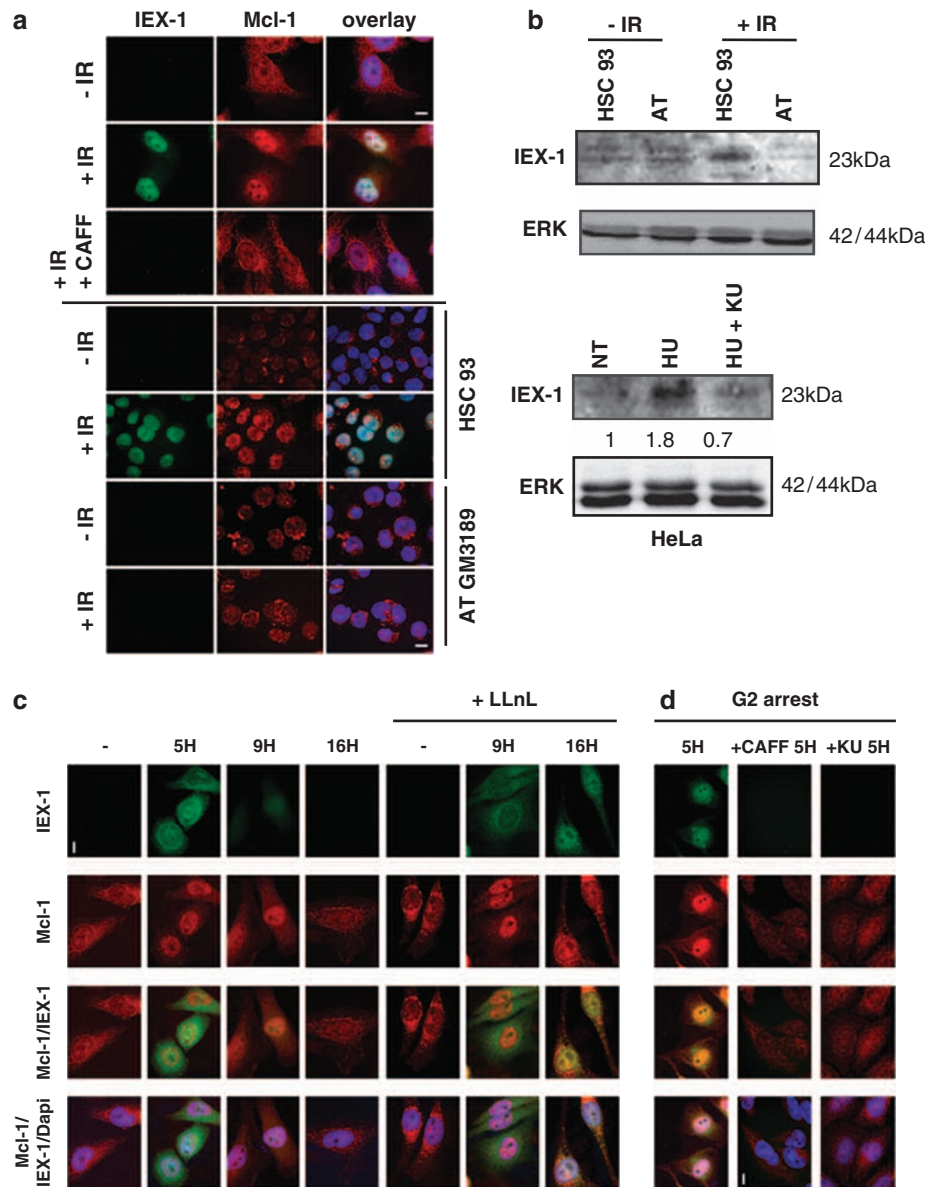
Figure 3 IEX-1 expression and degradation are controlled by ATM activity. (**a**, **b**) HeLa cells or the lymphoblastic cell lines HSC93 (WT) and AT GM3189 were IR or treated with HU. After 2–4 h, the cells were either stained for IEX-1 (green) and Mcl-1 (red) (**a**) or lysed and analyzed by IB (**b**). Where indicated, 3 mM caffeine was added 30 min before treatment. Quantification of IEX-1 levels is shown relative to the level of IEX-1 in non-treated cells, after normalization to ERK levels. (**c**) HeLa cells were treated overnight with HU (1.5 mM) and released in fresh medium. LLnL (25 μM) or vehicle alone was added 5 h later and the incubation was pursued for 4 or 11 h (9 and 16 h total time). Exponentially growing cells treated or not for 4 h with LLnL were used as controls. At the indicated times, the cells were fixed and stained for IEX-1 (green) and Mcl-1 (red). Nuclei were counterstained with DAPI. (**d**) HeLa cells were synchronized in G1/S by double thymidine block, released in medium for 6 h and IR (10 Gy). At 16 h after IR, caffeine (3 mM) or KU-55933 (10 μM) was added or not and IEX-1 and Mcl-1 expression were analyzed by IF 5 h later. Bars, 10 μm

shIEX-1 and shMcl-1 together (Figure 6d). This shows that the ability of IEX-1 to affect the DDR requires association with Mcl-1 and its translocation to the nucleus.

We then determined the region of Mcl-1 involved in IEX-1 binding. Truncation of the C-terminal 20 amino-acids of Mcl-1 (ΔCter), encoding the transmembrane region, abolished its interaction with IEX-1 (Figure 7a). Mcl-1 WT, but not ΔCter, could fully restore DNA repair as well as Chk1 phosphorylation in Mcl-1$^{-/-}$ MEFs (Figures 7b and c). However, Mcl-1 WT was unable to restore the rapid disappearance of γ-H2AX foci of Mcl-1$^{-/-}$ MEFs in which IEX-1 expression had been

knocked down by IEX-1 shRNAs (Figure 7d). Altogether, these results show that IEX-1 and Mcl-1 require each other and act on a unique pathway to regulate the DDR.

IEX-1- or Mcl-1-deficient cells show genomic instability. Mcl-1$^{-/-}$ MEFs and IEX-1$^{-/-}$ progenitors showed increased sensitivity to IR, relative to their WT counterparts (Figures 8a and b). After IR or HU, up to 62% of shIEX-1- and shMcl-1-expressing cells presented micro or fragmented nuclei, which could be easily distinguished from apoptotic cells (Figure 8c). Spontaneous micronuclei were also observed
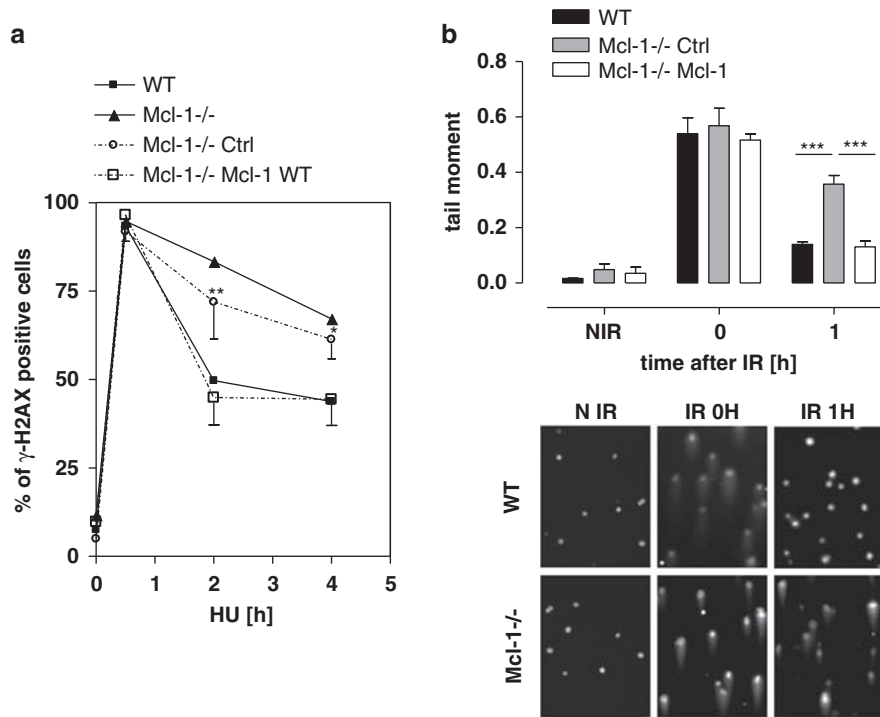
Figure 4 Mcl-1 deficient cells show increased DNA damage. (**a**) WT and Mcl-1$^{-/-}$ MEFs infected with empty (Ctrl) or Myc-Mcl-1-expressing retroviruses were treated with HU (2 mM) for various times, and fixed and stained with anti-γH2AX antibody. Cells containing $\geqslant$10 foci were scored as positive. At least 250 cells were counted for each time point. Means and S.E.M. from three independent experiments are shown. (**b**) WT and Mcl-1$^{-/-}$ MEFs infected as above were irradiated (10 Gy) and transferred to agarose for comet assay, directly (0) or after 1 h of recovery. Tail moments were scored from at least 80 cells per point. Means $\pm$ S.E.M from three independent experiments and representative pictures are shown. *$P < 0.05$; **$P < 0.01$; ***$P < 0.001$

at a frequency slightly higher (1.4- to 2-fold) in these cells than in shControl-expressing cells. Other abnormalities, indicative of increased genomic instability, such as nuclear blebbing, multinucleation or unequal division, were also observed in the absence of IEX-1 or Mcl-1.

IEX-1-deficient mice also showed genomic instability. At 1 month after whole-body irradiation, metaphase spreads of cells isolated from IEX-1$^{-/-}$ bone marrows and spleens showed a significant increase in chromosomal aberrations when compared with controls (Figure 8d). Thus, the absence of IEX-1 leads to sustained DNA lesions in hematopoietic cells. However, no difference in survival between WT and IEX-1$^{-/-}$ mice was observed at that time, suggesting that compensatory mechanisms would limit the effect of this defect on irradiated organisms.

Discussion

Cell cycle arrest, survival and DNA repair are coordinately controlled in the face of DNA damage. Recent data have revealed the existence of unexpected direct interactions between checkpoint/repair components and members of the Bcl-2 family or other regulators of the apoptotic pathway. For example, Bid and APAF translocate to the nucleus and affect S-phase arrest after DNA damage,[25–27] and Bax and Bcl-2 negatively regulate homologous recombination.[28] In this study we show that Mcl-1 is an integral component of the DDR, in multiple types of primary and transformed cells, and in response to various stresses such as IR, genotoxic

agents or replication inhibitors. Cells lacking Mcl-1 show altered G2 checkpoint, leading to extended DNA damage and inefficient DNA repair. These defects translate into increased genomic instability and sensitivity in response to DNA damage.

DNA damage triggers a striking accumulation of Mcl-1 in the nucleus and its association with the chromatin. The signal regulating Bid function in DNA damage is provided by ATM phosphorylation.[25,27] The Mcl-1 protein sequence does not present ATM/ATR phosphorylation sites. We show that Mcl-1 nuclear accumulation and function upon DNA damage occurs in an ATM-dependent manner through a new mechanism involving its association with IEX-1. Indeed, (1) IEX-1 binds to Mcl-1 and triggers its nuclear accumulation; (2) Mcl-1 nuclear accumulation and induction of IEX-1 by DNA-damaging agents are concomitant and dependent on ATM activity; (3) DNA damage-induced Mcl-1 nuclear accumulation is blunted in IEX-1-deficient cells; and (4) IEX-1 and Mcl-1 are functionally interdependent, as IEX-1 or Mcl-1 expression cannot restore the DDR in a double IEX-1- and Mcl-1-deficient background. IEX-1 loss can fully reproduce the defects in G2 arrest and DNA repair of Mcl-1-deficient cells. Bone marrows and spleens of IEX-1$^{-/-}$ mice also presented signs of genomic instability 1 month after whole-body irradiation, showing that impeding Mcl-1 nuclear accumulation is biologically significant. IEX-1 serves as a signal for Mcl-1 nuclear entry and as an anchor to maintain it in the nucleus during the DDR. Indeed, Mcl-1 relocalization to the cytoplasm is concomitant to IEX-1 disappearance and is prevented upon
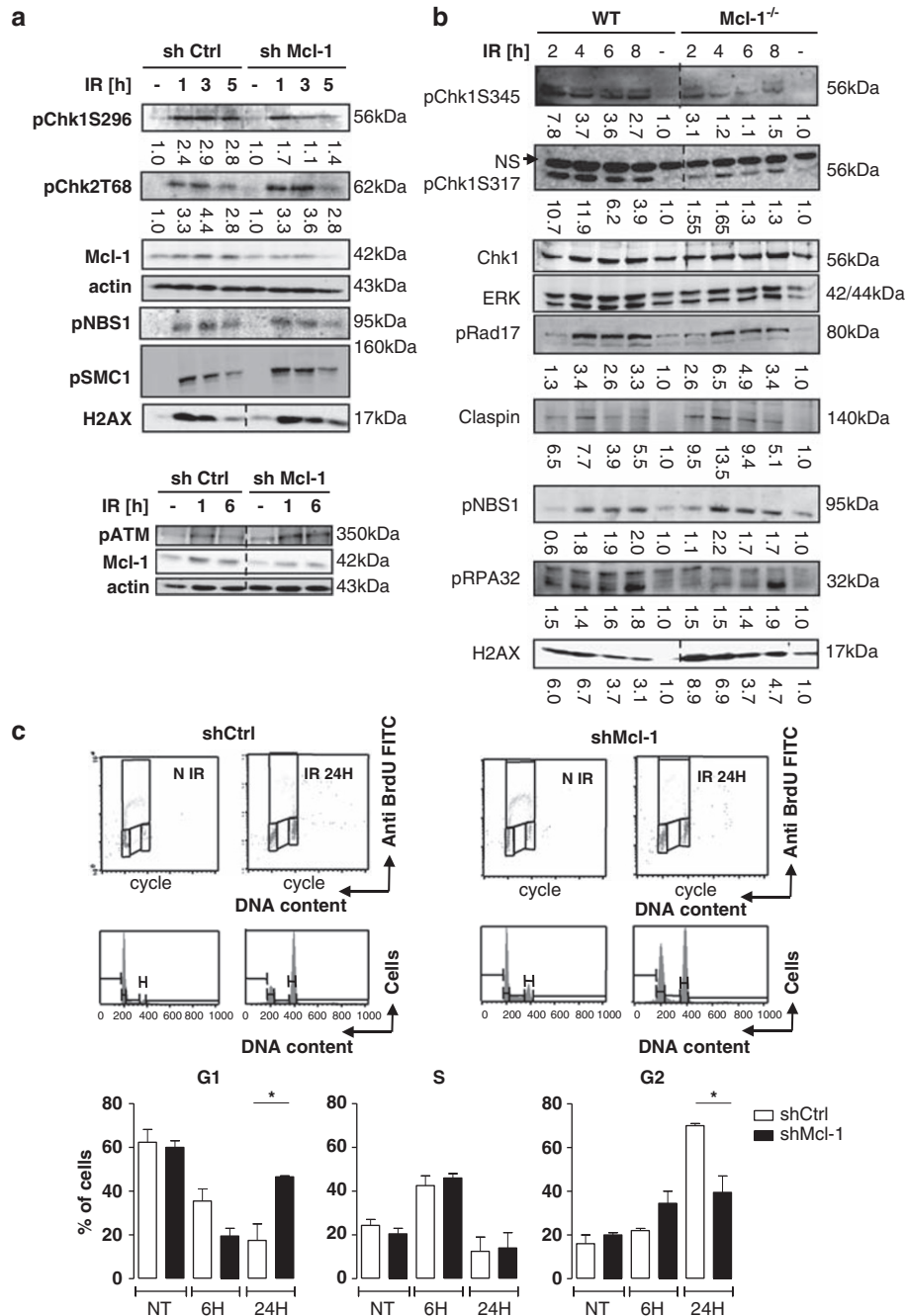
Figure 5 Mcl-1 deficient cells show impaired Chk1 activity and G2/M checkpoint. HeLa cells expressing control or Mcl-1 shRNAs (**a**, **c**) or Mcl-1$^{-/-}$ and Mcl-1$^{+/+}$ MEFs (**b**) were harvested at various times after IR (10 Gy). (**a**, **b**) Total lysates were analyzed by IB with the indicated antibodies. To avoid repeated stripping, the same samples were loaded several times on 6–15% acrylamide gels. All the results shown come from unique blots and exposures. Images were cutoff (dotted line) when the samples were not loaded side by side. Quantifications are expressed relative to the levels before IR, after normalization on actin (**a**) or ERK (**b**) levels. (**c**) The cells were incubated for 30 min with BrdU and fixed. After staining with antibodies to BrdU and with PI, the cells were analyzed using flow cytometry. Representative dot plots and mean ± S.E.M. from three independent experiments are shown. *$P < 0.05$

inhibition of IEX-1 degradation. Interestingly, IEX-1 degradation and Mcl-1 nuclear exit precede cell recovery from G2 arrest and re-entry into mitosis (Supplementary Figure S5-a). Silencing of checkpoint signaling, by adding ATM inhibitors after the cells were arrested in G2, accelerates IEX-1 degradation and Mcl-1 nuclear exit (Figure 3d), together with re-entry in mitosis (Supplementary Figure S5-b). Thus, both IEX-1 induction and degradation are DNA damage-sensed and ATM-dependent events. They represent a sensitive means to timely and specifically control the presence of
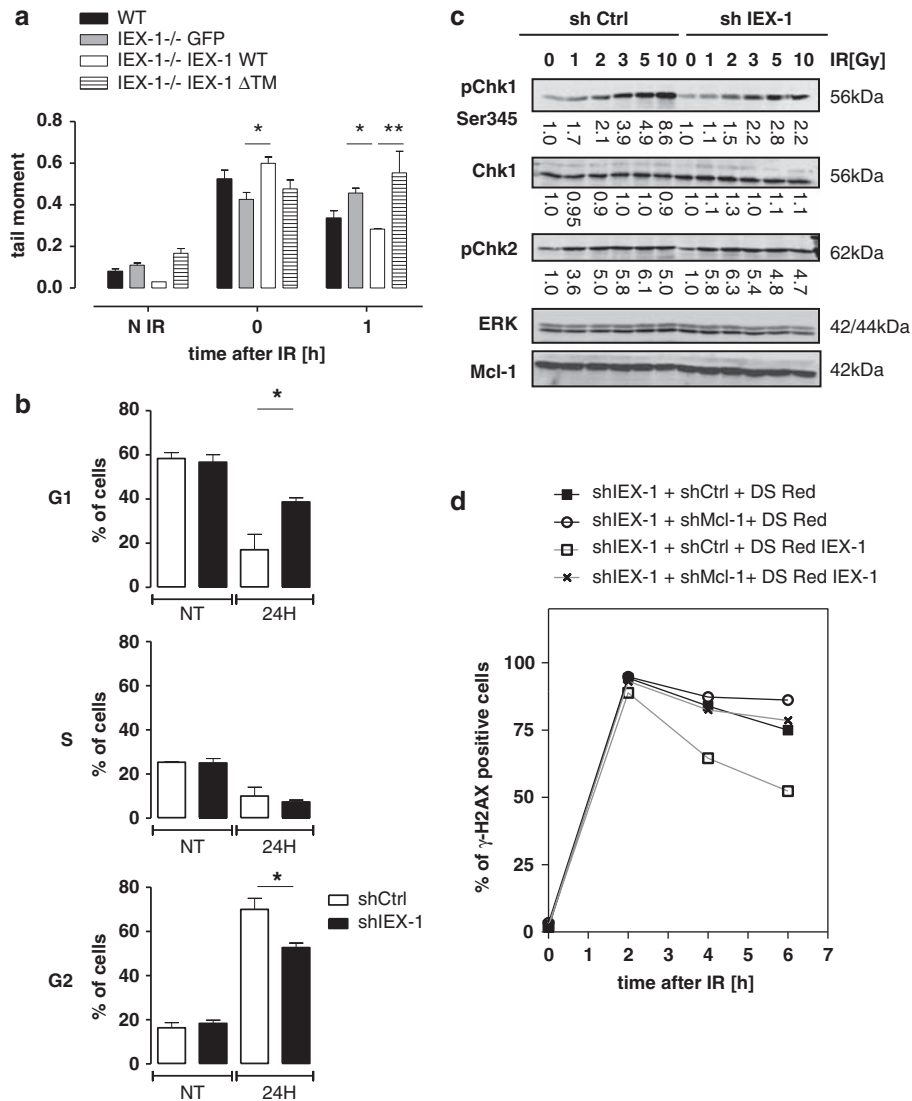
Figure 6 IEX-1 regulates DDR and this response requires interaction with Mcl-1. (**a**) WT MEFs, or IEX-1$^{-/-}$ MEFs infected with GFP- or with IEX-1 WT- or ΔTM-encoding vectors, were subjected to IR (10 Gy). Comet tail moments were scored as in Figure 4b. Results are means and S.E.M. from three independent experiments. (**b**) HeLa cells expressing shIEX-1 or control were irradiated and analyzed for cell cycle 24 h later as described in Figure 5c. Means and S.E.M. of three independent experiments are shown. (**c**) IB analysis of total lysates prepared from shRNA-expressing HeLa cells harvested 2 h after IR with the indicated doses. Quantifications are expressed relative to the levels at the zero time point, after normalization on ERK levels. (**d**) HeLa cells expressing shIEX-1 together with either shRNA control or shMcl-1 were infected with mIEX-1 or empty retroviruses. At 6 h after IR (10 Gy), the cells were fixed and stained with anti-γH2AX. Results are means from duplicate slides in which at least 250 cells were counted. *$P<0.05$; **$P<0.01$

Mcl-1 in the nucleus after DNA damage, allowing maintenance of the G2 arrest and its subsequent switch-off, authorizing the re-entry into the cell cycle.

Previous reports have shown that DNA damage can trigger a rapid decrease in Mcl-1 protein and/or mRNA levels, whereas others have reported the opposite results.[5,20,29] These discrepancies may be linked to the types of detergent used to prepare the lysates, as we show that Mcl-1 partially associates with chromatin after DNA damage and/or with the doses of DNA-damaging agents. We did not observe major change in Mcl-1 levels, upon DNA damage, overexpression or downregulation of IEX-1, indicating that IEX-1 alters only Mcl-1 subcellular localization. IEX-1, as Mcl-1, associates with mitochondria and endoplasmic reticulum

membranes.[15,16] IEX-1/Mcl-1 interaction requires their transmembrane domains. Thus, IEX-1 could bind to Mcl-1 in the mitochondrial membrane and then transport it to the nucleus. Supporting this possibility, IEX-1-ΔNLS was unable to induce Mcl-1 nuclear accumulation and the two proteins co-precipitated from both nuclear and cytosolic fractions. On the other hand, Mcl-1 is present at low levels in the nucleus in the absence of genotoxic stress.[8–10] Thus, although IEX-1 appears as a major mechanism controlling Mcl-1 nuclear accumulation upon DNA damage, Mcl-1 may transit to the nucleus independently of IEX-1 during the normal cell cycle. This result fits with previous reports showing that overexpression of Mcl-1 inhibits cell cycle progression in the absence of DNA damage.[9,10]
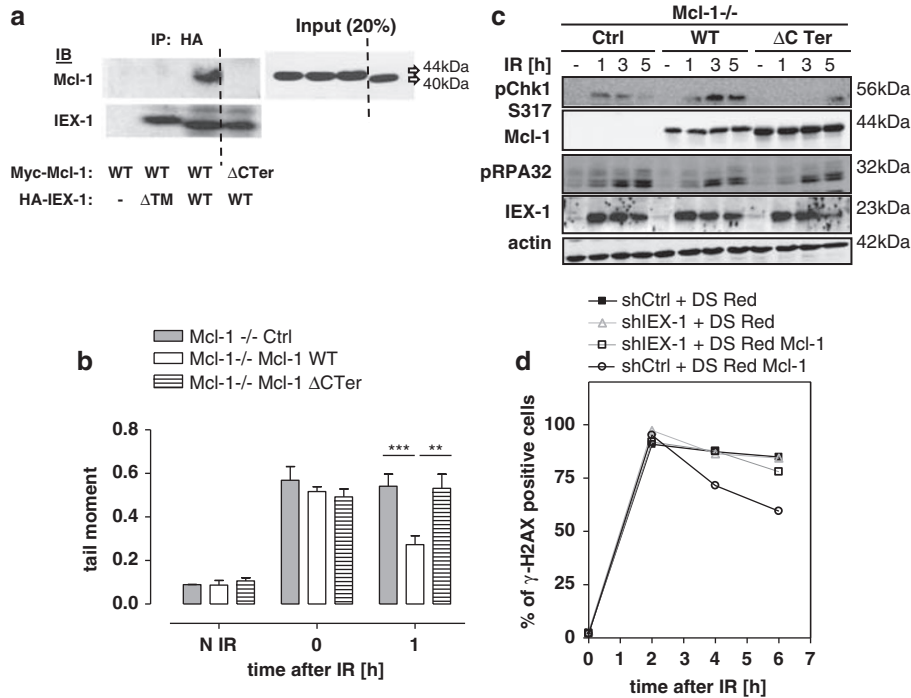
Figure 7 The ability of Mcl-1 to regulate DDR is dependent on IEX-1. (**a**) CHO cells were transiently transfected with HA-IEX-1 WT or ΔTM alone or with Myc-Mcl-1 WT or ΔCter mutant. Anti-HA immunoprecipitates were analyzed by IB. (**b**, **c**) Mcl-1^{−/−} MEFs infected with empty or myc-Mcl-1 WT or ΔCter-encoding viruses were irradiated (10 Gy) and harvested at different times for comet assays (**b**) or IB (**c**). (**b**) Means ± S.E.M. of three independent experiments. (**d**) Mcl-1^{−/−} MEFs expressing control or mIEX-1 shRNAs were subsequently infected with empty or WT Mcl-1-encoding vectors. At various times after IR, γH2AX foci were assessed. Results are means from duplicate slides in which at least 250 cells were counted. **$P < 0.01$; ***$P < 0.001$

The slow decrease in the comet tail moments in IEX-1- or in Mcl-1-depleted cells after irradiation suggests that these cells accumulate DSBs because of defects in DNA repair. However, their cell cycle arrest was not longer. In fact the opposite is observed. This suggests that IEX-1/Mcl-1 complexes have a major role in checkpoint signaling, at the level or downstream of the activation of the checkpoint kinases. Indeed, Chk1 activation was selectively impaired in the absence of IEX-1 or Mcl-1. This defect can explain why these cells accumulate DSBs;[30] however, how IEX-1 and Mcl-1 cooperate to maintain Chk1 activation is unknown. After IR, several proteins required for the DDR accumulate to chromatin in discrete foci, which are needed for activation of Chk1/Chk2.[1] Although Mcl-1 and IEX-1 partially associate with chromatin, they do not seem to participate to the recruitment of DDR proteins to foci. Indeed, soon after IR, γ-H2AX was normally enriched in foci in Mcl-1 or IEX-1-deficient cells. This is consistent with the fact that IEX-1 expression and Mcl-1 nuclear accumulation could be detected only approximately 30 min after IR. Neither the phosphorylation of ATM and its substrates (NBS1, SMC1 and Chk2) nor that of the ATR substrates (RPA and Rad17) required for Chk1 activation[30] was compromised in the absence of Mcl-1, suggesting that IEX-1/Mcl-1 complexes affect signaling downstream of ATM/ATR activation. Jamil et al.[20] have reported that etoposide induces a truncated form of Mcl-1 that associates with Chk1, but we were unable to reproduce these results. This might be because of the different antibodies or lysates conditions used. Claspin binds to Chk1

and ATR and is essential for Chk1 phosphorylation.[31] However, we could not precipitate Mcl-1 or IEX-1 with claspin. Claspin and Chk1 levels were not decreased in Mcl-1-deficient cells, showing that their degradation was not affected.[32–34] On the other hand, IEX-1 mutants, which were impaired in their ability to inhibit PP2A,[23] could restore the DDR of IEX-1^{−/−} MEFs (data not shown), suggesting that IEX-1/Mcl-1 do not maintain Chk1 activity by inhibiting its dephosphorylation by these phosphatases.[35]

In contrast with the apoptosis ensuing Mcl-1 mitochondrial degradation,[5] the delocalization of Mcl-1 to the nucleus upon DNA damage triggers DNA repair and checkpoint survival signals. IEX-1 depletion increases cell radiosensitivity while leaving intact the Mcl-1- mitochondrial pool. Thus, Mcl-1 function in the DDR requires its nuclear localization and is separately controlled from its activity at the mitochondria. Mcl-1 is overexpressed in many tumors and it is often responsible for the resistance to treatment with the BH3-mimetic ABT-737.[36] Cancer therapies involving DNA-damaging agents have the potential to induce IEX-1 expression and Mcl-1 nuclear localization, in which they may act together to foster checkpoint and improve the tumor resistance to DNA damage. Deciphering the pathways involved in IEX-1 degradation should lead to the discovery of new therapeutic targets to increase tumor cells sensitivity to chemotherapy.

Materials and Methods

Chemicals and antibodies. Hydroxyurea, the proteasome inhibitor LLnL, etoposide, caffeine, cytochalasin B and colcemid were purchased from Sigma
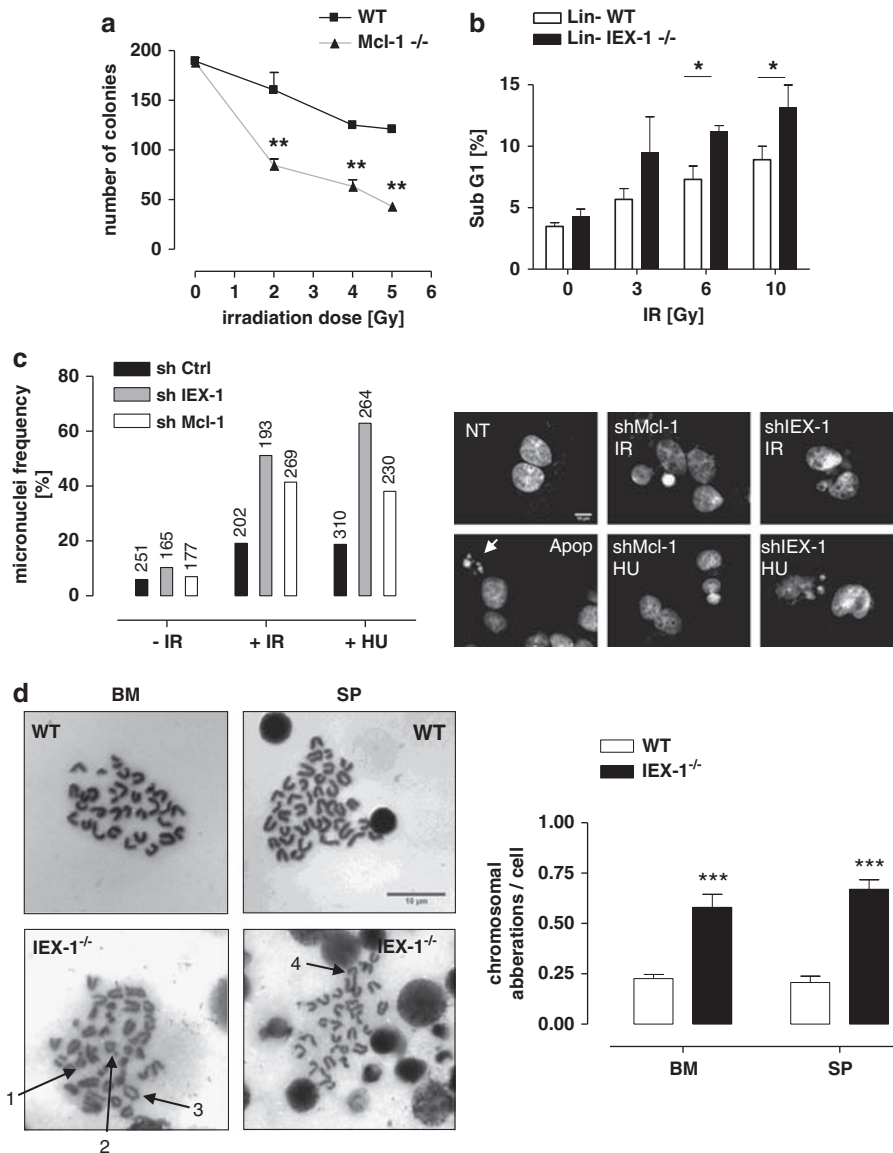
Figure 8 IEX-1- or Mcl-1-deficient cells show genomic instability and increased susceptibility to DNA damage. (**a**) WT and Mcl-1$^{-/-}$ MEFs were irradiated with the indicated doses and tested in clonogenic assays. Means ± S.D. of three independent experiments. (**b**) Lin$^-$ cells isolated from of WT and IEX-1$^{-/-}$ mice were irradiated at various doses and the subG1 fraction was determined by PI staining 16 h later. Results are means and S.E.M. from three different mice. (**c**) HeLa cells were exposed to IR (10 Gy) or HU (1.5 mM), incubated with cytochalasin B (2 μg/ml) for 24 h and then fixed and stained with DAPI. Binuclear cells were scored for micronuclei appearance. The number of cells scored for each point is indicated above the bars. Representative pictures show binuclear control cell (NT), micronuclei (shIEX-1, IR), multinucleation (shMcl-1, IR), nuclear blebbing (shIEX-1, HU), unequal division (shMcl-1, HU) and cell in apoptosis (Apop). (**d**) IEX-1$^{-/-}$ and IEX-1$^{+/+}$ mice were subjected to 7 Gy IR. The numbers of chromosomal breaks were evaluated in metaphase spreads of bone marrow (BM) and spleens (SP) 1 month later. Results are means ± S.E.M. of aberrations found in at least 30 metaphases from each of five WT and five IEX-1$^{-/-}$ mice for BM and three WT and five IEX-1$^{-/-}$ mice for SP. Arrows indicate chromatid break (1 and 2) and chromatid fusion (3 and 4). Bars, 10 μm. *$P<0.05$; **$P<0.01$; ***$P<0.001$

non-essential amino acids (NEAA, Invitrogen), 1% L-glutamine and 1% penicillin/streptomycin (PS). To obtain lineage-negative (Lin⁻) hematopoietic progenitors, bone marrow cells from 1- to 3-month-old mice were harvested from tibiae and femurs and depleted of lineage-positive cells using the Biotin-conjugated Mouse Lineage Panel of antibodies and magnetic beads (BD Pharmingen, San Jose, CA, USA). Immortalized WT and Mcl-1⁻/⁻ MEFs[2] were a generous gift from JT Opferman (St. Jude Children's Research Hospital, Memphis TN, USA). Cells were cultured in DMEM supplemented with 10% FCS, 1% NEAA, 1% L-glutamine, 1% PS and 0.1 μM β-mercaptoethanol. Chinese hamster ovary (CHO) and HeLa cells were cultured in Dulbecco's MEM Mix F-12 and DMEM, respectively, supplemented with 10% FCS. ATM WT (HSC93) and ATM-null (AT GM3189) human lymphoblasts were grown in RPMI medium with 12% FCS. All irradiation experiments were carried out using a Biobeam 8000 irradiator (Gamma Service Medical GmbH, Leipzig, Germany). All commercially available cell lines were from the American Type Culture Collection (ATCC, Manassas, VA, USA).

Plasmids, infections and transfections. IEX-1 constructs were described previously.[16,23] pcDNA-HA-IEX-1 deleted of its transmembrane domain (IEX-1-ΔTM) was generated by removing amino acids 86–101,[21] using QuickChange site-directed mutagenesis kit (Stratagene, La Jolla, CA, USA). IEX-1 WT and ΔTM were subcloned in pTRIPΔU3-EF1α-IRES-GFP[38] or in pRetro-x-IRES-DsRed (Clontech, Mountain View, CA, USA) lentiviral and retroviral vectors, respectively. pTRIPΔU3-EF1α-GFP encoding shRNAs against IEX-1 or controls (shScramble or shGFP) were previously described.[38] The vector encoding shRNA for murine IEX-1 was constructed as above using 5'-CATTGCCAAGAGGGTCCTC-3' (nucleotides 243–261) as the target sequence. pLL3.7 lentiviral constructs encoding three different shRNAs for Mcl-1 and GFP[39] were gifts from A Nencioni (MIT, Cambridge, MA, USA). Myc-Mcl-1 was provided by M-C Hung (University of Texas, MD Anderson Cancer Center, Houston, TX, USA). Myc-Mcl-1-ΔCter was made by deletion of amino acids 330–350 by adding a stop codon by PCR amplification. Myc-Mcl-1 WT and ΔCter cDNAs were then subcloned into pRetro-x-IRES-DsRed. Transient transfection of CHO and HeLa cells were performed with Lipofectamine (Invitrogen), as described.[23] Production and titration of retroviral and lentiviral particles and infections were performed as described.[38] The infection efficiency was assayed by testing DsRed or GFP expression using flow cytometry.

Immunoprecipitation and subcellular fractionation. Immunoprecipitation procedures were described previously.[23] For subcellular fractionation, cells were lysed in 10 mM HEPES, pH 7.9, 10 mM KCl, 1.5 mM MgCl₂, 0.34 M sucrose, 10% glycerol, 1 mM DTT, 10 mM NaF, 1 mM Na₂VO₃, 0.1% Triton X-100 and Roche protease inhibitor cocktail for 5 min at 4°C. After centrifugation (4 min, 1300 × g, 4 °C), the nuclear pellet was resuspended in 50 mM Tris pH 7.5, 137 mM NaCl, 0.5% NP-40, 10% glycerol, 1 mM EDTA, 1 mM Na₂VO₃, 20 mM NaF and 1 mM sodium pyrophosphate.

Immunofluorescence. Cells grown on glass coverslips were fixed with 3.7% paraformaldehyde (15 min at room temperature (RT)), washed with PBS and permeabilized with ice-cold methanol followed by incubation in blocking buffer (10% horse serum, 1% BSA for γ-H2AX and Mcl-1 or 0.3% BSA, 0.2% glycine for IEX-1) for 1 h at RT and with primary antibodies (in PBS with 0.1% Triton X-100) overnight in 4°C. Fluorescent-conjugated secondary antibody was then added for 1 h at RT. Nuclei were counterstained with DAPI. To detect chromatin-bound proteins, soluble proteins were pre-extracted with detergent before fixation: the cells were washed and incubated for 1 min at RT in 60 mM PIPES, 25 mM HEPES-KOH, pH 6.9, 10 mM EGTA, 2 mM MgCl₂ and 0.5% Triton X-100 and then fixed with ice-cold methanol for 5 min at −20°C, before staining, as above. All slides were visualized using Leica DMI 6000 microscope (Wetzlar, Germany) equipped with a 63 × 1.6 oil-immersion objective and a MicroMAX 1300Y camera (Princeton Instruments, Trenton, NJ, USA). Pictures were analyzed using ImageJ software (developed at the National Institute of Health, Bethesda, MD, USA).

Comet assay. Cells were mock-treated or irradiated at 10 Gy and were either transferred directly on ice or allowed to recover at 37°C for 1 h. Neutral comet assay was performed using the CometAssay kit (Trevigen Inc., Gaithersburg, MD, USA). After drying, slides were stained with Hoechst 33342 and comet tails were visualized by a fluorescent microscope Leica DMI 6000 and analyzed using TriTek CometScore software (Tritek Corp., Sumerduck, VA, USA).

Survival assay. For clonogenic survival assays, MEFs were irradiated with various doses, transferred to 10 cm diameter dishes and allowed to grow for 6 days (MEFs). The cells were then fixed with ice-cold methanol and stained with 0.5% Giemsa solution. Colonies containing > 50 cells were scored. Apoptosis of Lin⁻ progenitors was evaluated by measuring SubG1 DNA contents 16 h after IR, using Cytomix TM FC500, Beckman Coulter flow cytometer (Beckman Coulter France, Villepinte, France).

Genomic instability. Genomic instability in vitro was assessed by micronuclei appearance. Cells were incubated with cytochalasin B (2 μg/ml) for 24 h. After fixation and DNA staining with DAPI, binuclear cells were scored for micronuclei. To evaluate chromosomal aberrations after whole-body irradiation, IEX-1⁻/⁻ and age-matched control mice were exposed to IR (7 Gy). After 1 month, the mice were killed and bone marrow and spleen cell suspensions were prepared. Bone marrow cells were cultured in DMEM supplemented with 10% FCS. Splenocytes were resuspended in RPMI containing 12% FCS and concanavalin A (5 μg/ml). After 48 h, the cells were incubated in the presence of colcemid for 3 h, fixed, and metaphase spreads were prepared, as described.[40] At least 30 metaphases from each sample were scored for the presence of deletions, fusions and triradial chromatid chromosomal aberrations.

BrdU labeling and cell cycle analysis. 30 min before test time points, the cells were pulsed labeled with 30 μM BrdU (Invitrogen), washed and fixed in 70% ethanol. Staining with anti-BrdU antibody and PI was described previously[26] Samples were analyzed by flow cytometry using CellQuest software (BD Biosciences, le Pont de Claix, France).

Statistical analysis. Results were statistically evaluated using two-way ANOVA and Bonferroni comparison post-test or t-test using GraphPad PrismTM version 4.0 software (GraphPad Software Inc., San Diego, CA, USA). Results are shown as means ± S.E.M. and the value of $*P < 0.05$ was determined as significant, and of $**P < 0.01$ or $***P < 0.001$ as highly significant.

Conflict of interest

The authors declare no conflict of interest.

1. Bartek J, Lukas J. DNA damage checkpoints: from initiation to recovery or adaptation. *Curr Opin Cell Biol* 2007; **19**: 238–245.
2. Opferman JT, Letai A, Beard C, Sorcinelli MD, Ong CC, Korsmeyer SJ. Development and maintenance of B and T lymphocytes requires antiapoptotic MCL-1. *Nature* 2003; **426**: 671–676.
3. Opferman JT, Iwasaki H, Ong CC, Suh H, Mizuno S, Akashi K et al. Obligate role of anti-apoptotic MCL-1 in the survival of hematopoietic stem cells. *Science* 2005; **307**: 1101–1104.
4. Rinkenberger JL, Horning S, Klocke B, Roth K, Korsmeyer SJ. Mcl-1 deficiency results in peri-implantation embryonic lethality. *Genes Dev* 2000; **14**: 23–27.
5. Nijhawan D, Fang M, Traer E, Zhong Q, Gao W, Du F et al. Elimination of Mcl-1 is required for the initiation of apoptosis following ultraviolet irradiation. *Genes Dev* 2003; **17**: 1475–1486.
6. Yang T, Kozopas KM, Craig RW. The intracellular distribution and pattern of expression of Mcl-1 overlap with, but are not identical to, those of Bcl-2. *J Cell Biol* 1995; **128**: 1173–1184.
7. Cory S, Huang DC, Adams JM. The Bcl-2 family: roles in cell survival and oncogenesis. *Oncogene* 2003; **22**: 8590–8607.
8. Zhang D, Li F, Weidner D, Mnjoyan ZH, Fujise K. Physical and functional interaction between myeloid cell leukemia 1 protein (MCL1) and Fortilin. The potential role of MCL1 as a fortilin chaperone. *J Biol Chem* 2002; **277**: 37430–37438.
9. Fujise K, Zhang D, Liu J, Yeh ET. Regulation of apoptosis and cell cycle progression by MCL1. Differential role of proliferating cell nuclear antigen. *J Biol Chem* 2000; **275**: 39458–39465.
10. Jamil S, Sobouti R, Hojabrpour P, Raj M, Kast J, Duronio V. A proteolytic fragment of Mcl-1 exhibits nuclear localization and regulates cell growth by interaction with Cdk1. *Biochem J* 2005; **387**: 659–667.

11. Kumar R, Lutz W, Frank E, Im HJ. Immediate early gene X-1 interacts with proteins that modulate apoptosis. *Biochem Biophys Res Commun* 2004; **323**: 1293–1298.
12. Yoon S, Ha HJ, Kim YH, Won M, Park M, Ko JJ *et al.* IEX-1-induced cell death requires BIM and is modulated by MCL-1. *Biochem Biophys Res Commun* 2009; **382**: 400–404.
13. Arlt A, Grobe O, Sieke A, Kruse ML, Folsch UR, Schmidt WE *et al.* Expression of the NF-kappa B target gene IEX-1 (p22/PRG1) does not prevent cell death but instead triggers apoptosis in Hela cells. *Oncogene* 2001; **20**: 69–76.
14. Arlt A, Rosenstiel P, Kruse ML, Grohmann F, Minkenberg J, Perkins ND *et al.* IEX-1 directly interferes with RelA/p65 dependent transactivation and regulation of apoptosis. *Biochim Biophys Acta* 2008; **1783**: 941–952.
15. Shen L, Guo J, Santos-Berrios C, Wu MX. Distinct domains for anti- and pro-apoptotic activities of IEX-1. *J Biol Chem* 2006; **281**: 15304–15311.
16. Garcia J, Ye Y, Arranz V, Letourneux C, Pezeron G, Porteu F. IEX-1: a new ERK substrate involved in both ERK survival activity and ERK activation. *EMBO J* 2002; **21**: 5151–5163.
17. Mittal A, Papa S, Franzoso G, Sen R. NF-kappaB-dependent regulation of the timing of activation-induced cell death of T lymphocytes. *J Immunol* 2006; **176**: 2183–2189.
18. Zhang Y, Schlossman SF, Edwards RA, Ou CN, Gu J, Wu MX. Impaired apoptosis, extended duration of immune responses, and a lupus-like autoimmune disease in IEX-1-transgenic mice. *Proc Natl Acad Sci USA* 2002; **99**: 878–883.
19. Rocher G, Letourneux C, Lenormand P, Porteu F. Inhibition of B56-containing protein phosphatase 2As by the early response gene IEX-1 leads to control of Akt activity. *J Biol Chem* 2007; **282**: 5468–5477.
20. Jamil S, Mojtabavi S, Hojabrpour P, Cheah S, Duronio V. An essential role for MCL-1 in ATR-mediated CHK1 phosphorylation. *Mol Biol Cell* 2008; **19**: 3212–3220.
21. Kondratyev AD, Chung KN, Jung MO. Identification and characterization of a radiation-inducible glycosylated human early-response gene. *Cancer Res* 1996; **56**: 1498–1502.
22. Kruse ML, Arlt A, Sieke A, Grohmann F, Grossmann M, Minkenberg J *et al.* Immediate early gene X1 (IEX-1) is organized in subnuclear structures and partially co-localizes with promyelocytic leukemia protein in HeLa cells. *J Biol Chem* 2005; **280**: 24849–24856.
23. Letourneux C, Rocher G, Porteu F. B56-containing PP2A dephosphorylate ERK and their activity is controlled by the early gene IEX-1 and ERK. *EMBO J* 2006; **25**: 727–738.
24. van Vugt MA, Bras A, Medema RH. Polo-like kinase-1 controls recovery from a G2 DNA damage-induced arrest in mammalian cells. *Mol Cell* 2004; **15**: 799–811.
25. Kamer I, Sarig R, Zaltsman Y, Niv H, Oberkovitz G, Regev L *et al.* Proapoptotic BID is an ATM effector in the DNA-damage response. *Cell* 2005; **122**: 593–603.
26. Zermati Y, Mouhamad S, Stergiou L, Besse B, Galluzzi L, Boehrer S *et al.* Nonapoptotic role for Apaf-1 in the DNA damage checkpoint. *Mol Cell* 2007; **28**: 624–637.
27. Zinkel SS, Hurov KE, Ong C, Abtahi FM, Gross A, Korsmeyer SJ. A role for proapoptotic BID in the DNA-damage response. *Cell* 2005; **122**: 579–591.
28. Dumay A, Laulier C, Bertrand P, Saintigny Y, Lebrun F, Vayssiere JL *et al.* Bax and Bid, two proapoptotic Bcl-2 family members, inhibit homologous recombination, independently of apoptosis regulation. *Oncogene* 2006; **25**: 3196–3205.
29. Zhan Q, Bieszczad CK, Bae I, Fornace Jr AJ, Craig RW. Induction of BCL2 family member MCL1 as an early response to DNA damage. *Oncogene* 1997; **14**: 1031–1039.
30. Chen Y, Sanchez Y. Chk1 in the DNA damage response: conserved roles from yeasts to mammals. *DNA Repair (Amst)* 2004; **3**: 1025–1032.
31. Lee J, Kumagai A, Dunphy WG. Claspin, a Chk1-regulatory protein, monitors DNA replication on chromatin independently of RPA, ATR, and Rad17. *Mol Cell* 2003; **11**: 329–340.
32. Mailand N, Bekker-Jensen S, Bartek J, Lukas J. Destruction of claspin by SCFbetaTrCP restrains Chk1 activation and facilitates recovery from genotoxic stress. *Mol Cell* 2006; **23**: 307–318.
33. Peschiaroli A, Dorrello NV, Guardavaccaro D, Venere M, Halazonetis T, Sherman NE *et al.* SCFbetaTrCP-mediated degradation of claspin regulates recovery from the DNA replication checkpoint response. *Mol Cell* 2006; **23**: 319–329.
34. Zhang YW, Otterness DM, Chiang GG, Xie W, Liu YC, Mercurio F *et al.* Genotoxic stress targets human Chk1 for degradation by the ubiquitin-proteasome pathway. *Mol Cell* 2005; **19**: 607–618.
35. Leung-Pineda V, Ryan CE, Piwnica-Worms H. Phosphorylation of Chk1 by ATR is antagonized by a Chk1-regulated protein phosphatase 2A circuit. *Mol Cell Biol* 2006; **26**: 7529–7538.
36. van Delft MF, Wei AH, Mason KD, Vandenberg CJ, Chen L, Czabotar PE *et al.* The BH3 mimetic ABT-737 targets selective Bcl-2 proteins and efficiently induces apoptosis via Bak/Bax if Mcl-1 is neutralized. *Cancer Cell* 2006; **10**: 389–399.
37. Sommer SL, Berndt TJ, Frank E, Patel JB, Redfield MM, Dong X *et al.* Elevated blood pressure and cardiac hypertrophy after ablation of the gly96/IEX-1 gene. *J Appl Physiol* 2006; **100**: 707–716.
38. Hamelin V, Letourneux C, Romeo PH, Porteu F, Gaudry M. Thrombopoietin regulates IEX-1 gene expression through ERK-induced AML1 phosphorylation. *Blood* 2006; **107**: 3106–3113.
39. Nencioni A, Hua F, Dillon CP, Yokoo R, Scheiermann C, Cardone MH *et al.* Evidence for a protective role of Mcl-1 in proteasome inhibitor-induced apoptosis. *Blood* 2005; **105**: 3255–3262.
40. Naim V, Rosselli F. The FANC pathway and BLM collaborate during mitosis to prevent micro-nucleation and chromosome abnormalities. *Nat Cell Biol* 2009; **11**: 761–768.

Supplementary Information accompanies the paper on Cell Death and Differentiation website (http://www.nature.com/cdd)